Harmonic Analysis on the Korean AC Railway System

Hanmin Lee*, Gildong Kim, Kwanghae Oh***, Gilsoo Jang† and Saehyuk Kwon******

Abstract - Line constants of the catenary system are estimated. The harmonic current that the Korean Train Express (KTX) injects into the catenary is measured to precisely analyze the harmonic effects. The Korean high-speed railway system is modeled by estimated and measured results. The system model is applied for predicting the harmonic effects. The simulation results from the system model are compared to field test data concerning the total harmonic distortion (THD). The reliability of the system model is verified.

Keywords: Catenary system, Harmonics, Korean high-speed railway

1. Introduction

The AC electric railway has progressed rapidly in Korea. Korea joined the league including France, Japan, Germany and Spain with the historical opening of its express rail in April 2004. Namely, Korea entered into the super high-speed train era, operating its trains at the speed of 300km/h, finally reaching its target speed of 350km/h (actually touching 352.4km/h) with high-speed train (HSR-350x). HSR-350x boasts its construction with 92 percent of local technology ranging from its unique design to core devices such as propulsion and control systems.

Modern AC electric cars have typically used thyristor or Pulse Width Modulation (PWM)-controlled converters, which give rise to higher harmonics. Harmonic currents in electric trains are one of the most important aspects of power quality. A load current model to represent electric trains was proposed [1]. The current harmonics injected from the AC electric car are propagated through power feeding circuits. As the feeding circuit is composed of resistance (R), inductance (L), and capacitance (C), the capacitance and the inductance of the feeding circuit on the side of the power system may cause a parallel resonance and an amplification of harmonic current at a specific frequency. Therefore, an exact assessment of the harmonic current flow must be undertaken during the designing and planning stage for the electric traction system [2-4]. Since the harmonic current flows through the catenary system, it needs to be accurately modeled to analyze and assess the harmonic effect on the power feeding system.

The electric railway system as well as the electric train was modeled. The electric railway system was expressed by a 2-port or 4-port network model [5, 6]. Also, filters to reduce harmonics were studied on the electric railway system [7-10].

In this paper, Line constants of the catenary system are estimated. The harmonic current that the KTX injects into the catenary is measured to precisely analyze the harmonic effects. The Korean high-speed railway system is modeled by estimated and measured results. Modeling for each railway system is performed by an 8-port network model that is an extension of the 2-port network theory.

The system model is applied for predicting the harmonic effects. The simulation results of the system model are compared to field test data pertaining to the total harmonic distortion (THD).

2. Korean high-speed railway system

The Korean high-speed railway systems are based on single-phase 55 kV / 27.5kV. They are connected to a 3-phase power system to be supplied with a large 1-phase load. AC feeding circuits supply electric trains with electric power through a 3-phase to a 2-phase Scott-transformer through feeders, contact wires and rails. Autotransformers are installed at approximately every ten kilometers with circuit breakers, which connect adjacently up and down tracks at the parallel post. Substations are located roughly every fifty kilometers, and there is a sectioning post midway between two substations. The SP has circuit breakers, which enable one feeding circuit to electrically separate from the other. They may be closed in case the adjacent SS is out of service. Fig. 1 shows a typical AC electric railway system.

† Corresponding author: Department of Electrical Engineering, Korea University, Korea. (gjang@korea.ac.kr)
* Korea University / Advanced EMU Research Team, Korea Railroad Research Institute, Korea. (hanmin@krri.re.kr)
** Advanced EMU Research Team, Korea Railroad Research Institute, Korea. (gdkim@krri.re.kr)
*** Information System Standards Division, Korea Agency for Technology and Standards, Korea. (khoh@ats.go.kr)
**** Department of Electrical Engineering, Korea University, Korea. (shkwon@elec.korea.ac.kr)
Received April 22, 2005 ; Accepted July 21, 2005

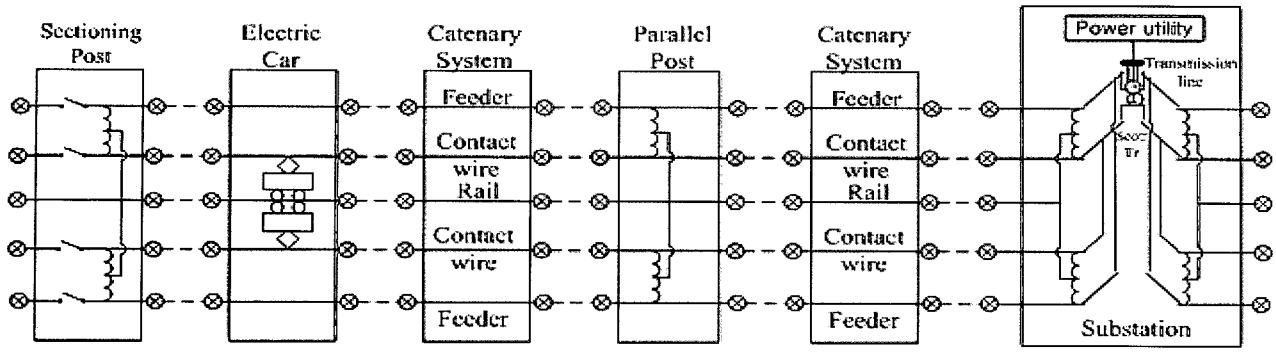

Fig. 1 Korean high-speed railway system

Fig. 2 is the Korean AC electric railway system model by the PSCAD/EMTDC, and it includes each subsystem module.

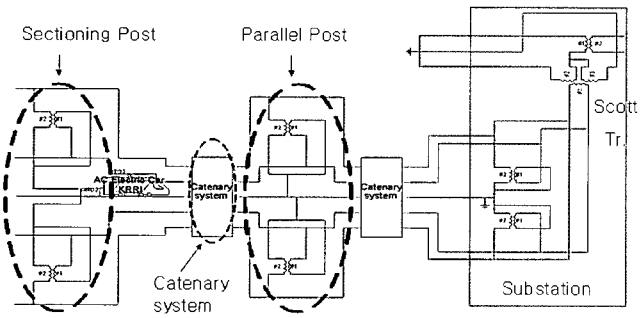

Fig. 2 Korean AC electric railway system model by the PSCAD/EMTDC

2.1 Formulation by 8-port representation

In a general way, desirable harmonic analysis should be performed on a 2-port representation for the sake of calculation convenience.

The harmonic current source is, however, connected to a contact line and rail conductor on the secondary sides of two autotransformers of which the primary terminals are linked between the contact line and the feeder in the circuit model as shown in Fig. 1. Moreover, there are capacitive admittances among three conductors (contact line, feeder and rail conductor). They make it impossible to realistically model the power feeding system upon a 2-port representation.

For that reason, this paper proposes a new model for harmonic analysis in the power supply system including feeders, contact lines, rails and autotransformers. The system model is based on an 8-port representation that is an extension of the 2-port network theory.

2.2 Catenary system

The catenary system has several conductors with a complex geometry, and the geometry is illustrated in Fig. 3. The system could consist of contact wires (4, 6), messenger wires (3, 5), feeders (1, 2), rails (7, 8, 9, 10), protection wires (11, 12), and buried earth wires (13, 14). Droppers every few meters connect two conductors such as the contact wire and the messenger wire. Those conductors are electrically regarded as one conductor. This simplification is made possible by the continuous parallel connection of some conductors. Finally, we can reduce the overall conductors to the equivalent of 5 conductors [11].

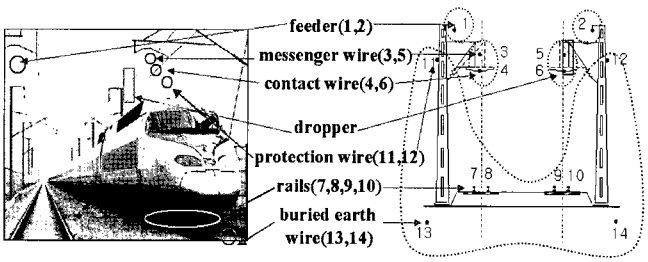

Fig. 3 Configuration of the catenary system

2.2.1 Impedance reduction method

All impedances are calculated using Carson equations.

The self-impedance per unit length is expressed by the following formula:

$$Z'_{ii} = Z_{Aii} + Z_{Eii} \tag{1}$$

where,

Z_{Aii} : Internal impedance per unit length of a conductor

Z_{Eii} : External impedance per unit length of a conductor with earth return

The elements of the series impedance matrix can then be calculated from the geometry of the catenary configuration and characteristics of the conductors. The mutual impedance is calculated by Eq. (2).

$$Z'_{ik} = Z'_{ki} = \Delta R'_{ik} + j(\omega \frac{\mu_0}{2\pi} \ln \frac{D_{ik}}{d_{ik}} + \Delta X'_{ik}) \tag{2}$$

with μ_0 = permeability of free space. Eq. (3) makes impedances in Ω/km.

$$\frac{\mu_0}{2\pi} = 2 \cdot 10^4 H/km \tag{3}$$

The parameters in Eqs. (2) and (3) are as follows:

D_{ik} : Distance between conductor i and the image of conductor k,

d_{ik} : Distance between conductor i and k,

ω : $2\pi f$ with frequency in Hz,

$\Delta R', \Delta X'$: Carson's correction terms for earth return effects.

Some conductors of the catenary system are regarded as one conductor electrically, and the conductors (n_{th} and $n\text{-}1_{th}$) become equal to one equivalent conductor as in Fig. 4.

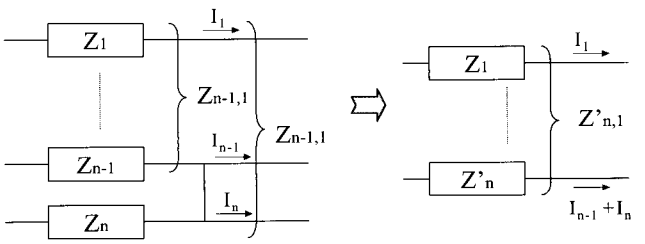

(a) (b)

Fig. 4 Equivalencing impedance of the catenary system

The equivalent impedance of Fig. 4(a) can be expressed as Eq. (4).

$$\begin{bmatrix} V_1 \\ \vdots \\ V_{n-1} \\ V_n \end{bmatrix} = \begin{bmatrix} Z_{1,1} & Z_{1,2} & \cdots & Z_{1,n} \\ \vdots & \vdots & \vdots & \vdots \\ Z_{n-1,1} & \cdots & \cdots & Z_{n-1,n} \\ Z_{n,1} & \cdots & \cdots & Z_{n,n} \end{bmatrix} \begin{bmatrix} I_1 \\ \vdots \\ I_{n-1} \\ I_n \end{bmatrix} \tag{4}$$

By the reduction method, the reduced equivalent impedances of Fig. 4(b) are expressed as Eq. (5).

$$\begin{bmatrix} V_1 \\ \vdots \\ V_{n-1} \end{bmatrix} = \begin{bmatrix} Z_{1,1}' & \cdots & Z_{1,n-1}' \\ \vdots & \vdots & \vdots \\ Z_{n-1,1}' & \cdots & Z_{n-1,n-1}' \end{bmatrix} \begin{bmatrix} I_1 \\ \vdots \\ I_{n-1}+I_n \end{bmatrix} \tag{5}$$

where

$$Z_{1,1}' = Z_{1,1} - \frac{(Z_{n-1,1}-Z_{n,1})(Z_{1,n-1}-Z_{1,n})}{Z_{n-1,n}+Z_{n,n}-2\times Z_{n-1,n}}$$

$$Z_{n-1,n-1}' = Z_{n-1,n-1} - \frac{(Z_{n-1,n-1}-Z_{n,n-1})(Z_{n-1,n-1}-Z_{n-1,n})}{Z_{n-1,n}+Z_{n,n}-2\times Z_{n-1,n}}$$

$$Z_{1,n-1}' = Z_{1,n-1} - \frac{(Z_{n-1,n-1}-Z_{n,n-1})(Z_{1,n-1}-Z_{1,n})}{Z_{n-1,n}+Z_{n,n}-2\times Z_{n-1,n}}$$

$$Z_{n-1,1}' = Z_{1,n-1}'$$

2.2.2 Capacitance reduction method

The conductors of the catenary system are affected through capacitive coupling. Modeling equivalent capacitance is identical to the process of the impedance reduction method. The feeder, the contact wire and the messenger wire are indicated in Fig. 5.

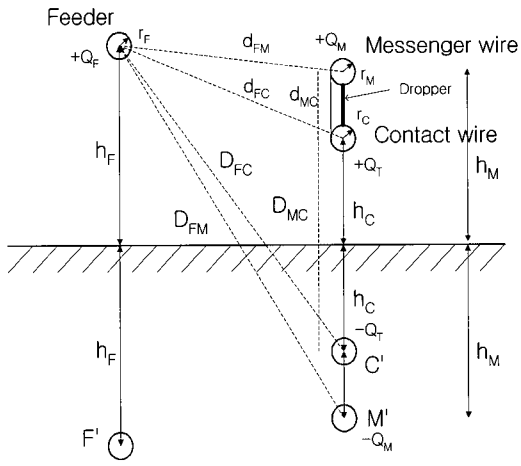

Fig. 5 Index for charge and potential calculation

The voltages from 3 conductors are a function of the line charge.

$$\begin{bmatrix} V_F \\ V_C \\ V_M \end{bmatrix} = \begin{bmatrix} P_{FF} & P_{FC} & P_{FM} \\ P_{CF} & P_{CC} & P_{CM} \\ P_{MF} & P_{MC} & P_{MM} \end{bmatrix} \begin{bmatrix} Q_F \\ Q_C \\ Q_M \end{bmatrix} \tag{6}$$

where,

Q = charge per unit length on conductor

$$P_{ii} = \frac{1}{2\pi\varepsilon_0} \ln \frac{2h_i}{r_i}, \quad P_{ij} = P_{ji} = \frac{1}{2\pi\varepsilon_0} \ln \frac{D_{ij}}{d_{ij}}$$

By the reduction method, the equivalent potential coefficients are calculated.

$$\begin{bmatrix} V_F \\ V_C \end{bmatrix} = \begin{bmatrix} P_{FF}' & P_{FC}' \\ P_{CF}' & P_{CC}' \end{bmatrix} \begin{bmatrix} Q_F \\ Q_C+Q_M \end{bmatrix} \tag{7}$$

Where

$$P_{FF}' = P_{FF} - \frac{(P_{CF}-P_{MF})(P_{FC}-P_{FM})}{P_{CC}+P_{MM}-2*P_{MC}}$$

$$P_{CC}' = P_{CC} - \frac{(P_{CC}-P_{MC})(P_{CC}-P_{CM})}{P_{CC}+P_{MM}-2*P_{MC}}$$

$$P_{FC}' = P_{FC} - \frac{(P_{CC}-P_{MC})(P_{FC}-P_{FM})}{P_{CC}+P_{MM}-2*P_{MC}}$$

$$P_{CF}' = P_{FC}'$$

Finally, we can obtain equivalent capacitances.

$$Q = CV, \quad C = P^{-1} \tag{8}$$

All values for impedances are evaluated using the Carson equations. The equivalent 5 conductors are calculated by the reduction method. The reduced catenary system is composed by PSCAD/EMTDC.

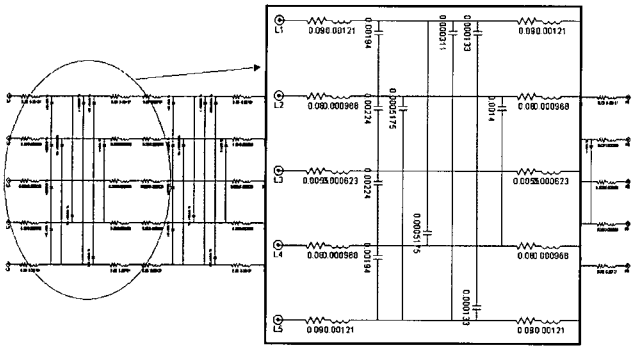

Fig. 6 Detailed model of the Catenary system

2.3 Harmonics source

We analyzed the measurement data of the harmonic current on the test track of the Korean high-speed railway system for the field test. The field test was performed in the KTX and in the substation (Shinchungju)

2.3.1 Power consumption of KTX

The characteristics of the power consumption of the KTX and those of the harmonic occurrence are tested in the KTX. The voltage that is the potential difference between the pantograph and the rail is measured through the PT. The current is measured through the CT of the circuit that supplies the current to 3 Motor Blocks.

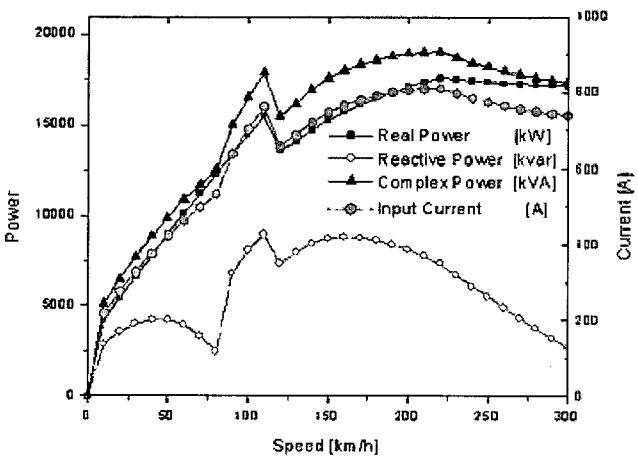

Fig. 7 Characteristic of power consumption of KTX

According to the speed of the KTX, the detailed results of the power consumption are indicated in Fig. 7.

The power consumption is peaked at 200 km/h. The special characteristics of the curves appear at about 100km/h. This phenomenon is due to the additional injection of the Power Factor Compensator (PFC).

2.3.2 Characteristic of KTX

The KTX is put in front of a substation to exclude the effect of line constants of the catenary system. The KTX is isolated from the adjacent power system. We operated 6 Motor Blocks and recorded the characteristics of the harmonics. Therefore, the complete circuit is:

Power utility - transmission line - scott-transformer - autotransformer - KTX.

The measured waveform of the voltage and the current is illustrated in Fig. 8.

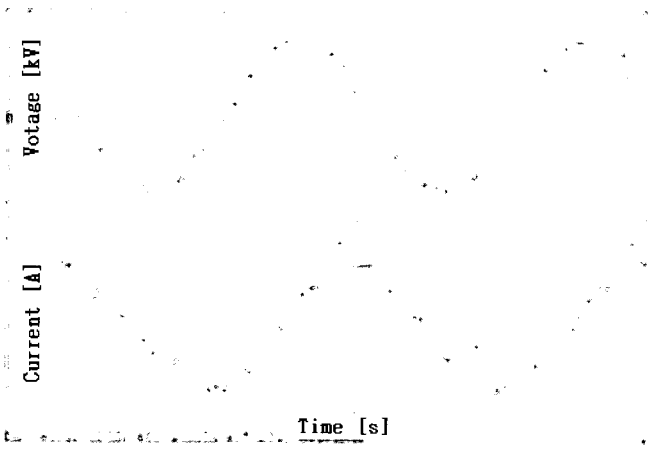

Fig. 8 Waveform of voltage (up) and current (down)

A harmonic current source in the AC electrified railway system is, mainly, the electric train. It can be considered as a harmonic current source injected from rail to contact line as shown in Fig. 9.

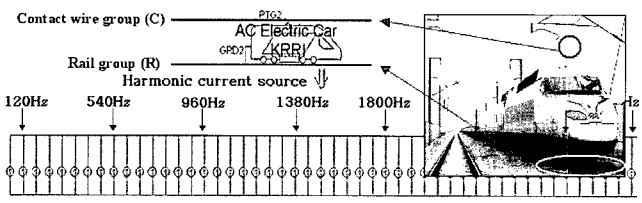

Fig. 9 Harmonic current source

2.4 Autotransformer

The autotransformer is placed between the catenary and the adjacent feeder with the rails connected to the center point on the winding. The AC electric railway system supplies 55 kV between the contact wire and the feeder with the autotransformer of ratio 1 : 1 (feeder-rail : rail-contact wire) to step down the high voltage 55 kV to 27.5 kV. Autotransformers are installed approximately every 10

kilometers along the railroad. The equivalent circuit of the autotransformer is presented in Fig. 10.

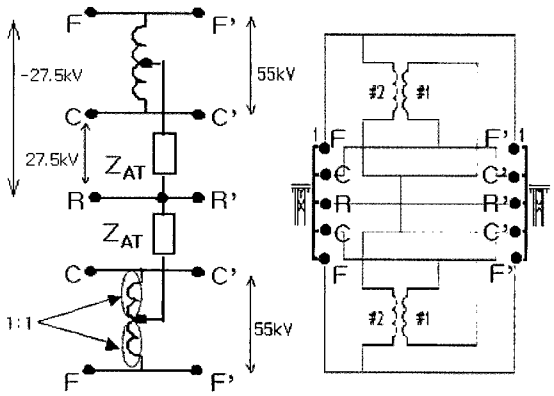

Fig. 10 Autotransformer

2.5 Power supply

As shown in Fig. 11, the power utility supplies 154 kV to the AC electric railway system through transmission lines. The scott-transformer in the substation steps down from 154 kV to 55 kV. Two pairs of 1-phase power are obtained from a scott-transformer. The turn ratios of T-phase and M-phase are $\sqrt{3}N_1/2:N_2$ and $N_1:N_2$ respectively. It is assumed that E_A, E_B, and E_C are pure 60 Hz sinusoidal voltage sources for the harmonic analysis.

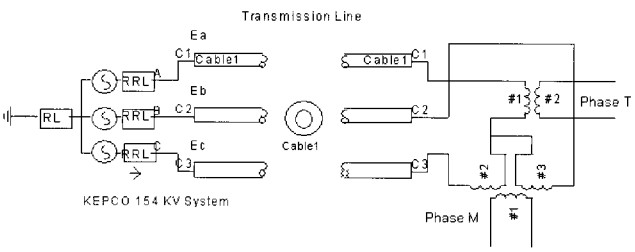

Fig. 11 Power supply system

The connection diagram of windings in the scott-transformer is depicted in Fig. 12.

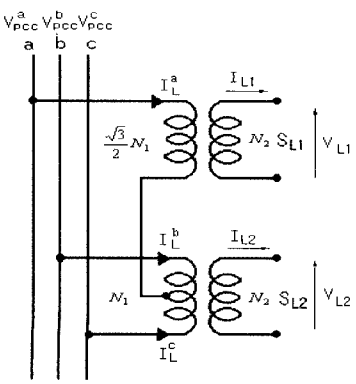

Fig. 12 Scott-transformer

3. Case study

3.1 Amplification of harmonic current

In order to verify the proposed model and observations, we have analyzed and tested the Korean high-speed railway system focusing on the amplification of the harmonic current. Fig. 13 illustrates the harmonic current with respect to the electric train location. We changed the location of the electric train from the substation (0 km) to 30 km. All the resonance frequency is occurred at the 24th order, even when the location of the electric train is changed. The resonance frequency does not depend on the location of the electric train as shown in Fig. 13. The amplification of the harmonic current is, however, a function of the position of the electric train. The farther the electric train is from the substation, the higher the amplification of the harmonic current is. Fig. 14 illustrates the correlation between the catenary length and harmonic resonance. From the result, we found that the longer the catenary length is, the lower the resonance frequency is.

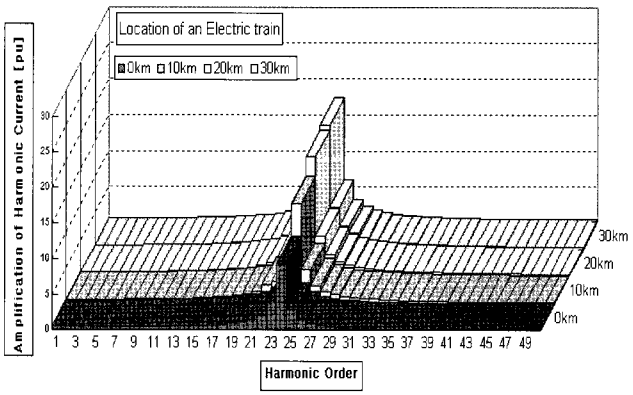

Fig. 13 Amplification of current harmonic as a function of the position of an electric train

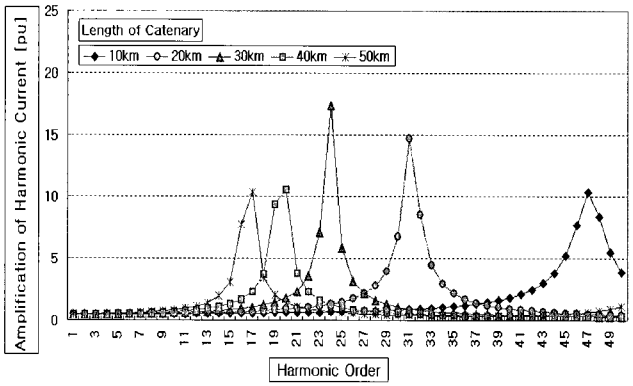

Fig. 14 Correlation between the catenary length and harmonic resonance

These phenomena are analyzed by the following formula.

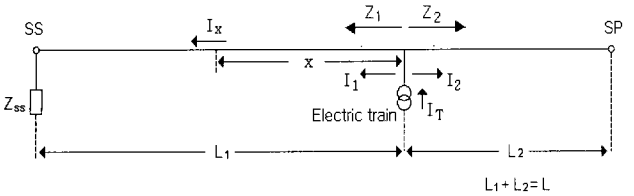

Fig. 15 Contact lines diagram

From Fig. 15, we can write the following formula.

$$I_T = I_1 + I_2 \tag{9}$$

$$I_1 = I_T \cdot \frac{Z_2}{Z_1 + Z_2 + \frac{Z_1 \cdot Z_2}{Z_T}} \tag{10}$$

$$I_2 = I_T \cdot \frac{Z_1}{Z_1 + Z_2 + \frac{Z_1 \cdot Z_2}{Z_T}} \tag{11}$$

where,

I_T : Current of the electric train

I_1 : Contact line current towards the substation

I_2 : Contact line current towards the end of the line

Z_1 : Contact line input impedance towards the substation and seen from the electric train

Z_2 : Contact line input impedance towards the end of the supply section and seen from the electric train

Z_T : Internal impedance of the electric train

$$Z_1 = Z_0 \cdot \frac{Z_{SS}\cosh\gamma L_1 + Z_0 \sinh\gamma L_1}{Z_{SS}\sinh\gamma L_1 + Z_0\cosh\gamma L_1}(\Omega) \tag{12}$$

$$Z_2 = Z_0 \cdot \frac{\cosh\gamma L_2}{\sinh\gamma L_2}(\Omega) \tag{13}$$

where,

L_1 : Distance between the electric train and the substation

L_2 : Distance between the electric train and the end of the feeder section

Z_{SS} : Resultant impedance of the feeder substation

Z_0 : Characteristic impedance of the contact line

γ : Unit length propagation constant of the contact line

Z_1 and Z_2 are composed as the parallel circuit by the electric train. The parallel impedance, Z_P, is expressed by the following formula:

$$Z_P = \frac{Z_0\cosh\gamma(L-L_1)\cdot(Z_{SS}\cosh\gamma L_1 + Z_0\sinh\gamma L_1)}{Z_{SS}\sinh\gamma L + Z_0\cosh\gamma L}(\Omega) \tag{14}$$

When the denominator is zero at Eq. (14), the circuit becomes the condition of resonance, then the harmonic current is amplified. And the resonance frequency is independent of the location of the electric train.

When the electric train is located at the end of line (SP), the condition is as follows.

$$L_2 = 0,\ I_1 = I_{SP},\ I_X = I_{SS} \text{ and } X = L \tag{15}$$

Finally, the amplification of harmonic current is expressed by the following equation.

$$K = \frac{I_{SS}}{I_{SP}} = \frac{Z_0}{Z_{SS}\sinh\gamma L + Z_0\cosh\gamma L}(pu) \tag{16}$$

Therefore, the farther the electric train is from the substation, the higher the amplification of harmonic current is.

Fig. 16 is a simple railway system with the power utility to analyze the resonance phenomenon.

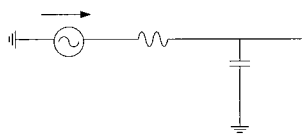

Fig. 16 The railway system for the resonance phenomenon

The relations of current and voltage are represented by the next equation (17).

$$I = \frac{V}{Z} = \frac{V}{jwL + \frac{1}{jwC_1}} \tag{17}$$

When this system becomes a resonance, Impedance, Z, is expressed by the following equation (18).

$$Z = 0,\ \omega^2 = \frac{1}{LC_1} \tag{18}$$

Therefore, the longer the catenary length is, the lower the resonance frequency is.

Finally, we obtained the amplification of the harmonic current on the Korean high-speed railway system by applying the reduced line constants. We simulated and measured the amplification of the harmonic current on the sections, which are Shinchungju-Yongjung and Pyongtaek-Maha. The distance of those sections is as follows:

- Shinchungju-Yongjung: 28.59 km
- Pyongtaek-Maha: 21.32 km

Results of the harmonic resonance simulation are presented in Figs. 17 and 18.

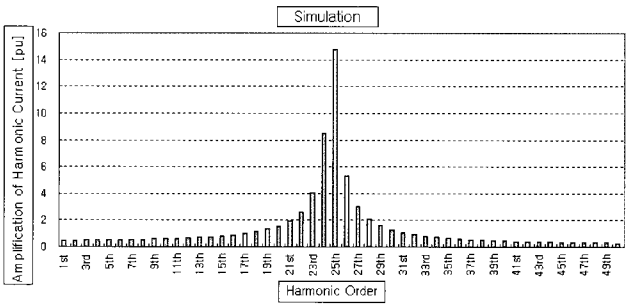

Fig. 17 Amplification of harmonic current (Shinchungju-Yongjung 28.59km)

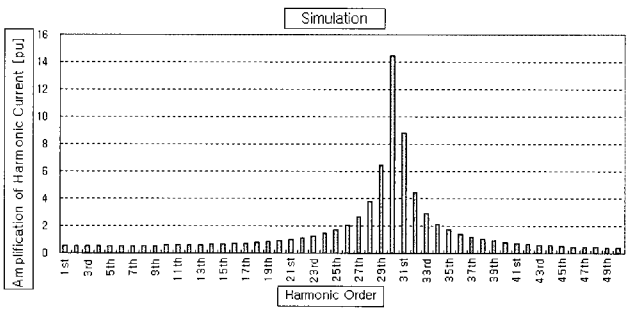

Fig. 18 Amplification of harmonic current (Pyongtaek-Maha 21.32km)

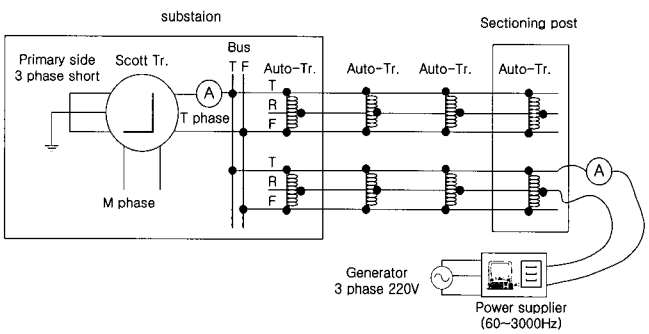

Fig. 19 Test for the amplification of harmonic currents

The harmonic current measurement is performed in the field in order to compare the simulation results with the measurement data focusing on the amplification of the harmonic current. We injected the currents from 60 Hz to 3000 Hz at the sectioning post and then measured these at the substation. The amplification of the harmonic current is measured from 60 Hz to 3000 Hz. The amplification of the harmonic current is calculated as the ratio of data at the sectioning post over data at the substation. The scheme for the measuring test is shown in Fig. 19. The results are compared in Table 1 and Fig. 20. The simulation results and the measurement data are almost identical. It verifies that the proposed harmonic model is well in accordance with the Korean high-speed railway system.

Table 1 Results of simulation and measurement of harmonic resonance according to catenary length

Distance	Classification	Resonance Harmonic Order
21.32km	Simulation	30th order
	Measurement	30th order
28.59km	Simulation	25th order
	Measurement	24th order

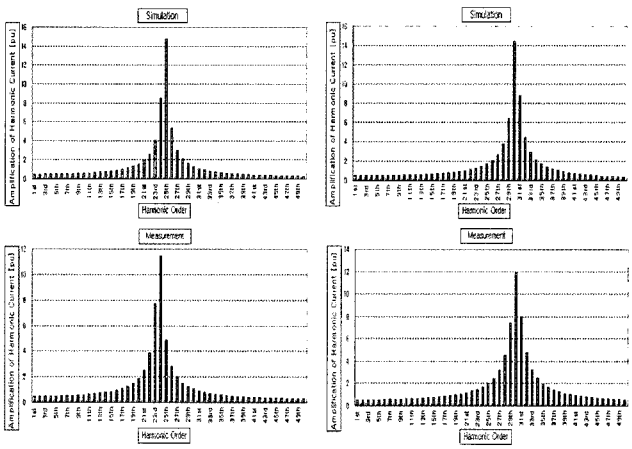

(a) Shinchungju-Yongjung-28.59 km (b) Pyongtaek-Maha-21.32 km

Fig. 20 Comparison of simulation results and measurement data

3.2 Comparison of THD

Since the THD is used as a standard for harmonics regulation, the THD is calculated as a harmonics assessment index for the Korean high-speed railway system. The THD of the voltage in the Korean railway system needs to be regulated within 1.5%. Since the THD varies depending on where it is calculated, it was calculated with 1 high-speed electric train set in operation on the Shinchungju-Yongjung section. Fig. 21 shows the calculation results at different assessing points where the Shinchungju railway substation 55 kV feeder bus and 154 kV incoming bus (KORAIL S/S), and the power utility's Chungwon substation 154 kV outgoing bus (KEPCO S/S) are located.

According to Fig. 21, the THD at Shinchungju railway substation is larger than the power utility's Chungwon substation 154 kV outgoing bus. This is because the harmonic impedances and the harmonic voltages at the Shinchungju railway substation are larger. Since the THD varies depending on the point of common coupling (PCC), the PCC of the THD should be defined. The electric power outgoing line (or point) is defined as the PCC in the analysis.

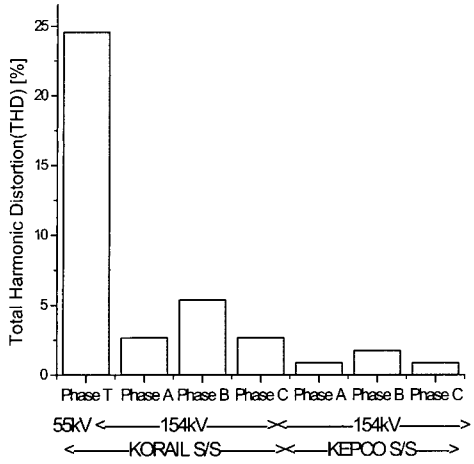

Fig. 21 Comparison of the THD at calculating points

In order to assess the harmonic performance of the Korean high-speed railway system with respect to electric train operation conditions, the THDs are calculated at the power utility's electric power outgoing lines. We perform simulation and measurement for the two cases. One is for 1 high-speed electric train operation. The other is for 2 high-speed electric trains. In case the operation condition is 1 high-speed electric train set, the maximum THD for the total operation period in the simulation is 2.1% as shown in Fig. 22. The maximum THD in the measurement is 1.95% as indicated in Fig. 23.

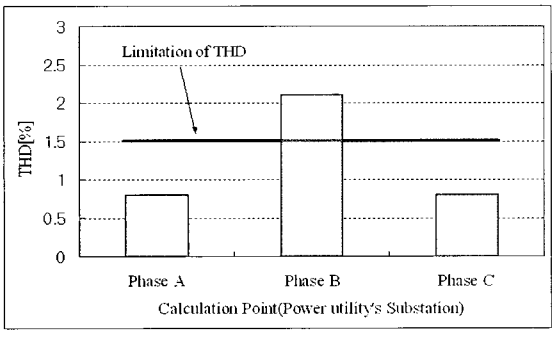

Fig. 22 The THDs of 1 high-speed electric train set operation (Simulation)

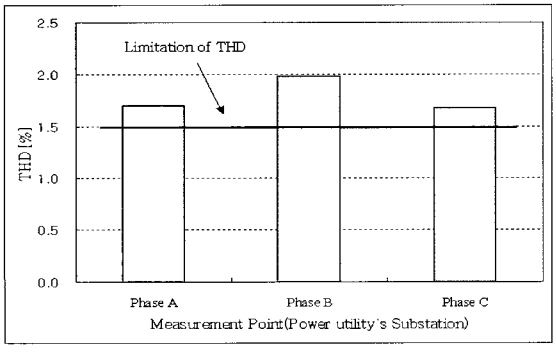

Fig. 23 Instantaneous and the maximum THDs of 1 high-speed electric train set operation (Measurement)

The following cases are for 2 high-speed electric trains. The maximum THD in the simulation is 2.5% as shown in Fig. 24. The maximum THD in the measurement is 2.3% as indicated in Fig. 25.

The simulation results for identifying the maximum THD value almost correspond to the measurement data, and they verify the capability of the proposed 8-port represented harmonic model.

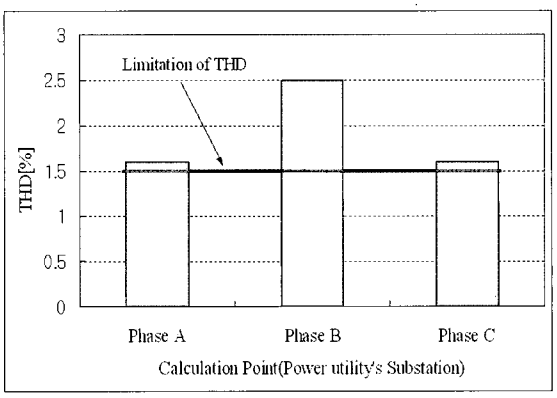

Fig. 24 The THDs of 2 high-speed electric trains(Simulation)

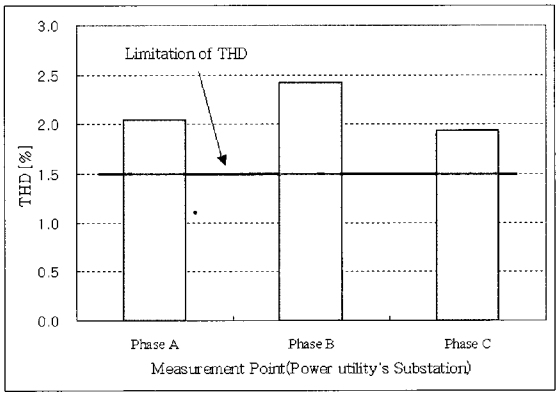

Fig. 25 The instantaneous and the maximum THDs of 2 high-speed electric trains (Measurement)

4. Conclusion

The model for the harmonic studies on the Korean high-speed railway system is presented. This study shows an approach to model and to analyze the system for the estimation of the amplification of the harmonic current and the THD.

The proposed model is based on the 8-port representtation that is an extension of the 2-port network theory. Aggregating subsystems compose the overall system.

Harmonic characteristics of the Korean high-speed railway system are presented. The harmonic effects on the Korean high-speed railway system according to operation conditions of the electric train are assessed.

In order to show the capability of the proposed model,

the model is simulated for estimating the characteristics of harmonics on the Korean high-speed railway system. The simulation results are presented in comparison with the actual measurement data to illustrate the validity of the proposed model.

References

[1] N J Balu, Railroad electrification on utility system: EPRI, EL-3001, Contract TPS 81-796, pp. 60-83, 1983.

[2] H Lee, C Lee, H Cho, G Jang, S Kwon, "Harmonic analysis model based on PSCAD/EMTDC for Korean high-speed railway", 2004 Large Engineering Systems Conference on Power Engineering, Halifax, Canada, July 2004.

[3] Yoshifumi Mochinaga, "Higher Harmonics Resonance on AT Feeding Circuit and Countermeasures to Suppress it", T.IEE Japan, Vol. 114-D, no. 10, 1994.

[4] J H Song, H M Hwang, "Estimation of Harmonics on Power System on AC Electric Railway", KIEE International Transactions on Power Engineering, Vol. 52B, No. 2, pp. 68-79, 2003.

[5]J Holtz, H J Klein, "The propagation of harmonic currents generated by inverter-fed locomotives in the distributed overhead supply system", IEEE Transaction on Power Electronics, Vol. 4, No. 2, pp. 168-174, 1989.

[6] R J Hill, I H Cevik, "On-line simulation of voltage regulation in autotransformer-fed AC electric railroad traction network", IEEE Transaction on Vehicular Technology, Vol. 42, No. 3, pp. 365-372, 1993.

[7]Peng, F.Z.; Akagi, H.; Nabae, A. "A new approach to harmonic compensation in power systems". Industry Applications Society Annual Meeting, pp. 874 - 880 Vol. 1, 1988.

[8] Yue Wang; Zhaoan Wang; Jun Yang; Jinjun Liu; Zhiping Fu; Yong Duan; Yahan Hua, "A novel comprehensive compensator for electrified railway system", Power Electronics Specialist Conference, Vol. 3, pp. 1032-1037, 2003.

[9] Jou, H.L.; Wu, J.C.; Chang, Y.J.; Feng, Y.T, "A Novel Active Power Filter for Harmonic Suppression", IEEE Transactions on Power Delivery. Vol. 20, pp. 1507–1513, 2005.

[10] Y S Jeon, K B Lee, B M Han, "Harmonics and Power Factor Controller for Single-Phase PWM Converter Using Two Input Sensors", KIEE International Transactions on Power Engineering, Vol. 53B, No. 10, pp. 618-624, 2004.

[11] CCITT, Directives concerning the protection of telecommunication lines against harmful effects from electric power and electrified railway lines: Vol. Ⅳ, 1989.

Hanmin Lee
He received his M.S. degree in Electrical Engineering from Korea University in 2000. He was part of the Electric Power Research Team at KRRI and also, the LRT System Development Team. Currently, he is a Researcher in the Advanced EMU Research Team.

Gildong Kim
He received his B.S degree in Electrical Engineering in 1986, M.S degree in 1991and Ph.D. from Myongji University in 2003. He was previously employed as a Researcher at the Shinkansen Inverter laboratory in Toshiba, Japan. Currently, he is Head of the Advanced EMU Research Team at KRRI.

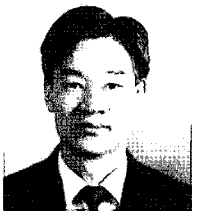

Kwanghae Oh
He received his Ph.D. from Korea University in 1996. He was previously a Leader in the Power System Research Group at KRRI. He is presently a Senior Researcher in the Information System Standards Division at the Korea Agency for Technology and Standards.

Gilsoo Jang
He received his Ph.D. from Iowa State University in 1997. He is presently an Associate Professor in the Department of Electrical Engineering at Korea University. His research interests include power quality and power system control.

Saehyuk Kwon
He received his M.S. and Ph.D. degrees in Electrical Engineering from Iowa State University. Currently, he is a Full Professor in the Department of Electrical Engineering at Korea University.